

IMPACT OF EUROPIUM CONCENTRATION ON THERMAL AND ABSORPTION FEATURES OF AMORPHOUS TELLURITE MEDIA

^{1,1} KHAIDZIR HAMZAH, ^{2,2*} AHMAD FARHAN SUFFIAN, ^{2,3} SIB KRISHNA GHOSHAL

¹Nuclear Engineering Programme, Faculty of Petroleum and Renewable Energy Engineering, Universiti
Teknologi Malaysia, 81310 UTM Johor Bahru, Johor, Malaysia.

²AOMRG, Department of Physics, Faculty of Science,
Universiti Teknologi Malaysia.

[1khaidzir@utm.my](mailto:khaidzir@utm.my), [2natkingcole90@gmail.com](mailto:natkingcole90@gmail.com), [3sibkrishna@utm.my](mailto:sibkrishna@utm.my).

*Corresponding author

Abstract. Improving the structural and optical properties of tellurite glasses via optimized doping of rare earth ions is an outstanding issue in materials science. Tellurite glasses doped with trivalent europium (Eu^{3+}) are successfully prepared using conventional melt quenching technique. Glasses with chemical composition of $(80-x)\text{TeO}_2-10\text{PbO}-10\text{ZnO}-(x)\text{Eu}_2\text{O}_3$ where $0 \leq x \leq 2.0$ mol% are obtained. The influence of Eu^{3+} ions concentration on the thermal and absorption properties of the synthesized glasses is investigated using Differential Thermal Analyzer (DTA) and UV-VIS Spectroscopy. DTA curves in the temperature range of 50-1000 °C at a heating rate of 10 °C/min are used to determine the temperature of glass transition, crystallization, melting and in turn the thermal stability. DTA revealed that the increase in the Eu^{3+} contents improved the thermal stability. This observation is attributed to the alteration of the glass network structure via the creation of non-bridging oxygen. The room temperature absorption spectra recorded in the spectral region of 200 – 2000 nm exhibited three absorption peaks corresponding to ${}^7\text{F}_0 \rightarrow {}^5\text{D}_0$, ${}^7\text{F}_0 \rightarrow {}^5\text{D}_1$ and ${}^7\text{F}_0 \rightarrow {}^5\text{D}_2$ transitions. The absorption intensity is found to be enhanced up to certain concentration of Eu^{3+} ions and then quenched. This is ascribed to the change in glass network structure and formation of defects through the cleavage of weak bonds and reduction in covalence states.

Keywords: Tellurite glass; UV-Vis absorption; nonbridging oxygen; quenching

1.0 INTRODUCTION

Tellurium oxide (TeO_2) based glasses are attractive due to their high efficiency for developing optical devices [1, 2]. The uses of tellurite as host material is ever increasing due to their potential in laser and fiber applications [3]. They possess low melting and glass transition temperature with high thermal stability. The resistive nature of tellurite glass to atmospheric moisture attack allows the incorporation of large concentration of rare-earth (RE) ions into the matrix [4]. RE ions play an important role in modern technology as optically active elements in solid state luminescence materials due to the energy levels possessed by these ions when incorporated into a solid state matrix. These RE doped glasses are promising for nonlinear optical devices because of their large third-order nonlinear optical susceptibility [5, 6]. Furthermore, Eu^{3+} doped tellurite glasses are widely used as a probe for finding the local structure around the RE ion in a crystal or a glass due to the relative simplicity of its energy level structure with non-degenerate ground $^7\text{F}_0$ and emitting $^5\text{D}_0$ states [7].

The determination of thermal and absorption properties is our specific interest. Following the conventional melt-quenching method, a series of Eu^{3+} doped lead and zinc-tellurite glasses are prepared to examine their thermal and optical features. The increment in the temperature of glass transition (T_g), crystallization (T_c) and glass stability (H_R) as a function of Eu_2O_3 concentration is demonstrated. The influence of RE ions on UV-Vis absorption and thermal properties are analyzed and the mechanism for modifications is understood.

2.0 EXPERIMENTAL

Series of Eu_2O_3 doped glasses with composition $(80-x)\text{TeO}_2-10\text{PbO}-10\text{ZnO}-(x)\text{Eu}_2\text{O}_3$ are synthesized using the melt-quenching technique. The glass compositions and their codes are summarized in Table 1. All the chemicals in the powder form are well-mixed and placed into the furnace at $900\text{ }^\circ\text{C}$ for complete melting. The melt is then poured into a steel mold and annealed at $350\text{ }^\circ\text{C}$ for 3 hours to reduce the mechanical stress.

Table 1: Nominal compositions of glass samples.

Samples	Compositions (mol %)			
	TeO_2	PbO	ZnO	Eu_2O_3
S1	80.0	10.0	10.0	0.0
S2	79.5	10.0	10.0	0.5
S3	79.0	10.0	10.0	1.0
S4	78.5	10.0	10.0	1.5
S5	78.0	10.0	10.0	2.0

DTA is conducted on Perkin Elmer DTA-7 Series System at a heating rate of $10\text{ }^\circ\text{C min}^{-1}$. Thermal properties such as T_g , T_c and thermal stability are determined from the tangent intersection on the enthalpy curve. The room temperature optical absorption measurement is performed in the

wavelength range of 200-1000 nm using UV-Vis-NIR spectrophotometer. The optical band gap (E_g) is estimated from Davis Mott equation and Tauc method using [8],

$$\alpha(\omega) = \frac{const}{\hbar\omega} (\hbar\omega - E_g)^n \quad (1)$$

where $\hbar\omega$ is the photon energy and α is the frequency (ω) dependent absorption coefficients. The value of E_g is obtained by extrapolating the linear part of the $(\alpha\hbar\omega)^{1/2}$ against phonon energy ($\hbar\omega$).

The defect states that originate from the conversion of weak bonds into defects are acquired from Urbach equation [9] using the expression,

$$\alpha(\omega) = B \exp\left(\frac{\hbar\omega}{\Delta E_u}\right) \quad (2)$$

where B is a constant and ΔE_u is the width of the band tail of the electron states. Urbach energy is evaluated from the slope of the plot of $\ln(\alpha)$ versus phonon energy ($\hbar\omega$).

3.0 RESULTS AND DISCUSSION

The DTA thermogram of all as synthesized samples is shown in Figure 1. The achieved values of T_g , T_c , and glass stability (H_R) are summarized in Table 2.

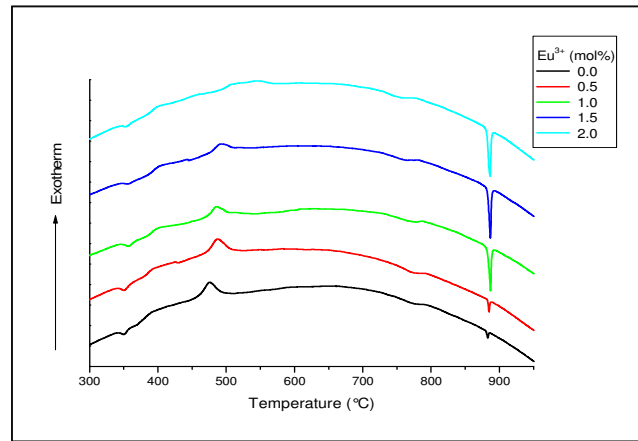


Figure 1: DTA patterns for $(80-x)\text{TeO}_2-10\text{PbO}-10\text{ZnO}-(x)\text{Eu}_2\text{O}_3$ glass system.

Table 2: Eu_2O_3 concentration dependent thermal parameters of all glass.

Sample	Er_2O_3 (mol %)	Temperature ($\pm 1^\circ\text{C}$)		
		T_g	T_c	H_R
S1	0.0	351	474	0.30

S2	0.5	351	487	0.34
S3	1.0	357	485	0.32
S4	1.5	359	493	0.34
S5	2.0	354	502	0.39

It is clear from Table 2 that T_g and T_c are increased from $351 \pm 1^\circ\text{C}$ to $354 \pm 1^\circ\text{C}$ and $474 \pm 1^\circ\text{C}$ to $502 \pm 1^\circ\text{C}$ as the Eu_2O_3 concentration increased from 0 to 2 mol%. A plot of T_g and T_c versus Eu^{3+} concentration is illustrated in Figure 2 and Figure 3, respectively. The value of T_g is found to be higher than the earlier observation which was $341 \pm 1^\circ\text{C}$ at 2.0 mol% of Eu_2O_3 [10]. The observed higher value of transition temperature with the increase of Eu_2O_3 content is ascribed to the increased rigidity of glass network due to the creation of non-bridging oxygen (NBO) atoms. These NBO forms the TeO_3 tp units via the intermediate coordination of TeO_{3+1} units [11]. However, the deviation from linearity at T_g and T_c is mainly due of the formation of heterogeneous nucleation sites in final stage of crystallization. The glass stability enhanced up to 0.39 as the Eu_2O_3 concentration is increased to 2 mol%.

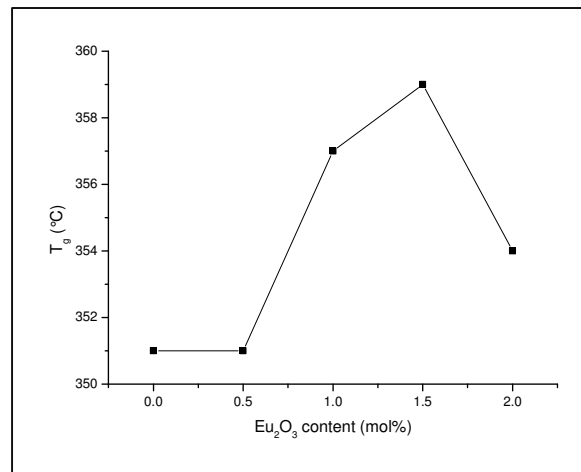


Figure 2: The Eu_2O_3 dopant concentration dependent T_g .

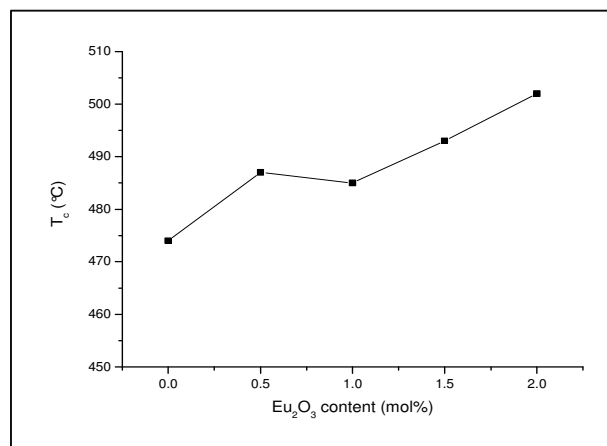


Figure 3: The dependences of T_c on the Eu_2O_3 dopant concentration.

The UV-Vis-NIR absorption spectra for all the glass samples is shown in Figure 4. It exhibits three prominent peaks centered around 461, 529 and 585 nm, which originate from the ground state (7F_0) to excited states (5D_0 , 5D_1 and 5D_2) transitions, respectively.

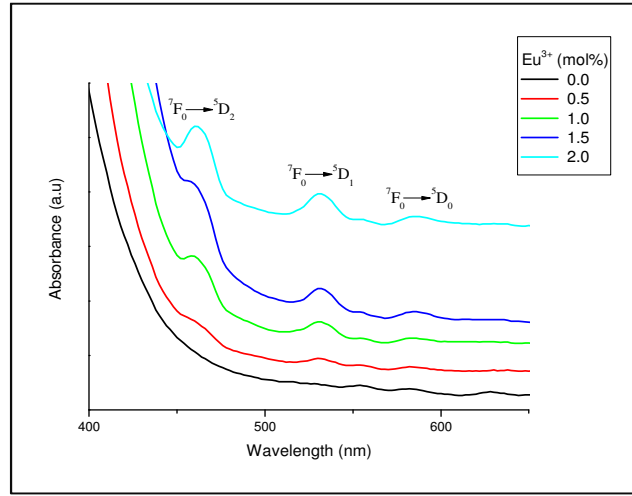


Figure 4: Absorption spectra of glasses for various concentration of Eu_2O_3 .

The values of Eu_2O_3 concentration dependent optical energy gap (E_g) and Urbach energy (E_u) calculated from the absorption spectra are listed in Table 3. Figure 5 and Figure 6 displays the Eu_2O_3 dependent variation of E_g and E_u . The value of E_g is found to increase from 2.89 to 3.01 eV as the Eu^{3+} content is increased from 0.5 to 2.0 mol%. The observed reduction in the band gap energies at higher concentration of Eu^{3+} ions is related to the structural changes in glass network arises from enhanced heat treatment time. The achieved value of E_g is comparable to the earlier observation on Te-based glass systems [12, 13]. Meanwhile, the value of E_u is found to decrease from 0.43 to 0.24 eV as the concentration of Eu^{3+} ions is increased.

Table 3: Optical band gap and Urbach energy for all prepared samples.

Samples	Eu_2O_3 Content (mol%)	Peak Transitions	Peak Wavelength (λ_p) (nm)	Band Gap Energy (E_g) (eV)	Urbach Energy (E_u) (eV)
S1	0.0	${}^7F_0 \rightarrow {}^5D_0$	585	2.89	0.43
S2	0.5			3.04	0.37
S3	1.0	${}^7F_0 \rightarrow {}^5D_1$	529	3.02	0.27
S4	1.5			3.00	0.25
S5	2.0	${}^7F_0 \rightarrow {}^5D_2$	461	3.01	0.24

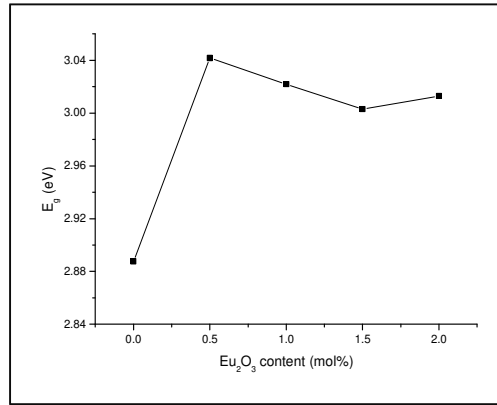


Figure 5: The Eu₂O₃ concentration dependent E_g.

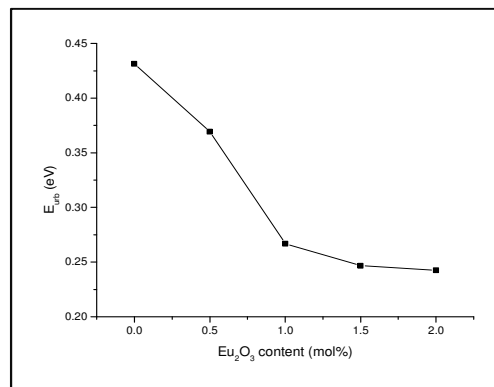


Figure 6: The Eu₂O₃ concentration dependent E_u.

4.0 CONCLUSIONS

The effects of Eu³⁺ contents on the thermal and absorption characteristics of (80-x)TeO₂-10PbO-10ZnO-(x)Eu₂O₃ are inspected. The temperature of glass transition, crystallization, melting and thermal stability is determined from DTA thermogram. The increase in the Eu³⁺ contents is found to improve the glass thermal stability. The changes of the glass network structure through the formation of non-bridging oxygen are primarily attributed to these modifications. The increase in absorption intensity and energy band gap up to certain concentration of Eu³⁺ ions and subsequent quenching at higher RE concentration is ascribed to the change in glass network structure and formation of defects via the breakage of weak bonds. We demonstrate the tunability of thermal and absorbance properties by varying Eu₂O₃ contents in the glass systems. This may be useful for optimization glass composition and the development of solid state lasers.

ACKNOWLEDGEMENTS

The authors gratefully acknowledge the financial support from UTM and Malaysian Ministry of Education through Vot.05H36 (GUP) and 4F424 (FRGS).

REFERENCES

- [1]. J.C. Sabadel, P. Armand, D. Cachau-Herreillat, P. Baldeck, O. Doclot, A. Ibanez, and E. Philippot, *Journal of Solid State Chemistry*, 1997. **132**(2): p. 411-419.
- [2]. Awang, A., S.K. Ghoshal, M.R. Sahar, M. Reza Dousti, R.J. Amjad, and F. Nawaz, *Current Applied Physics*, 2013. **13**(8): p. 1813-1818.
- [3]. S. Tanabe, K. Hirao, and N. Soga, *J.Non-Cryst.Solids*,, 1990: p. 122, 79.
- [4]. Y Nageno, H Takeke, and H. Morinaga, *J Amor Cer Soc*, 1993. **76**: p. 3081.
- [5]. Sazali, E.S., M.R. Sahar, S.K. Ghoshal, R. Arifin, M.S. Rohani, and A. Awang, *Journal of Alloys and Compounds*, 2014. **607**: p. 85-90.
- [6]. S. K. Ghoshal, M. R. Sahar, M. R. Dousti, R. Arifin, M. S. Rohani, and K. Hamzah, *Adv. Mat. Res.*, 2012. **501**(61).
- [7]. Babu, P., H.J. Seo, C.R. Kesavulu, K.H. Jang, and C.K. Jayasankar, *Journal of Luminescence*, 2009. **129**(5): p. 444-448.
- [8]. Naser M. Ahmed, Zaliman Sauli, Uda Hashim, and Y. Al-Douri, *Int. J. Nanoelectronics and Materials*, 2009 **2**: p. 189-195.
- [9]. M. Kranjċec, *Journal of Non-Crystalline Solids*, 2009. **355**: p. 54-57.
- [10]. M.R. Sahar and E.S. Sazali, UMTAS, 2011.
- [11]. Sahar, M.R., Penerbit Universiti Teknologi Malaysia, 1998.
- [12]. A. T. Adorno, R. A. G. Silva, and T.B. Neves, *Mat. Sc. Eng. A*, 2006. **441**: p. 259-265.
- [13]. E. B. Araujo and E. Idalgo, *Opt. Mat.*, 2011.